Journal of
ALLOYS
AND COMPOUNDS

An Interdisciplinary Journal
of Materials Science and
Solid-State Chemistry and Physics

Contents lists available at SciVerse ScienceDirect

Journal of Alloys and Compounds

journal homepage: www.elsevier.com/locate/jalcom

Novel ternary compound Ce$_2$RuAl: Synthesis, crystal structure, magnetic and electrical properties

E. Murashova [a],*, Zh. Kurenbaeva [a], A. Tursina [a], E. Marushina [a], A. Yaroslavtsev [b], D. Leshchev [b], Y. Seropegin [a], D. Kaczorowski [c]

[a] Department of Chemistry, Moscow State University, 119992 Moscow, Russia
[b] National Research Nuclear University "MEPhI", 115409 Moscow, Russia
[c] Institute of Low Temperature and Structure Research, Polish Academy of Sciences, 50-950 Wroclaw, Poland

ARTICLE INFO

ABSTRACT

The intermetallic phase Ce$_2$RuAl was synthesized by arc melting the elemental components and subsequent annealing of the product at 823 K. Its crystal structure was determined from the single-crystal X-ray diffraction data and confirmed by powder X-ray diffraction at room temperature. The compound is of a new structural type related to the LaF$_3$-type of structure: space group $P6_3cm$, $Z = 6$, $a = 7.8362(7)$ Å, $c = 9.7510(9)$ Å, Pearson symbol $hP24$. Some Ce–Ru distances in the unit cell are unusually short being equal to 2.4821(6) Å. This structural feature brings about instability in the cerium valence state, directly evidenced in the XANES data and corroborated in the study of bulk physical behavior in Ce$_2$RuAl.

1. Introduction

In the so far known aluminides with high aluminum content, like CeRu$_2$Al$_{10}$ [1], Ce$_2$Ru$_3$Al$_{15}$ [2], Ce$_3$Ru$_4$Al$_{12}$ [3], CeRu$_3$Al$_{10}$ [4], and Ce$_2$RuAl$_3$ [5,6], typical metallic bonds between cerium and ruthenium atoms (2.9–3.5 Å) are observed. In contrast, cerium-rich ternary compounds Ce$_5$Ru$_3$Al$_2$ [7], CeRuAl [8,9], Ce$_4$RuAl [10,11], and Ce$_{11}$Ru$_2$Al$_6$ [12] are characterized by very short Ce–Ru interatomic distances ranging from 2.440 to 2.803 Å, i.e. significantly smaller than the sum of the covalent radii of Ce and Ru that equals 2.89 Å [13]. These structural peculiarities are often accompanied by unusual physical properties at low temperatures, exemplified by intermediate valence (IV) behavior in the alluminide Ce$_5$Ru$_3$Al$_2$ [7]. Similar IV properties were reported for a few other Ce–Ru–X intermetallics with X = Ga, Mg, In, Sn, Zn, Cd, which also exhibit unusually short Ce–Ru contacts [14–26].

In the present paper, we report on the formation, crystal structure and physical properties of a novel ternary phase from the Ce–Ru–Al system, namely Ce$_2$RuAl. Alike the afore-mentioned Ce-rich materials, the new compound exhibits significant reduction of Ce–Ru interatomic distances, which is accompanied by distinct cerium valence instability.

2. Experimental

2.1. Synthesis

A polycrystalline sample of Ce$_2$RuAl was prepared by arc-melting the elemental constituents (purities: Ce 99.8 wt.%, Ru 99.99 wt.%, Al 99.999 wt.%) in argon atmosphere of 0.7×10^5 Pa. To ensure homogeneity, the ingot was turned over and re-melted. Subsequently, the button was sealed in an evacuated quartz ampoule and annealed at 823 K for 30 days. After the heat treatment the ampoule was quenched in cold water.

2.2. EDXS data

The sample composition was checked by energy-dispersive X-ray spectroscopy (EDXS) performed on a Carl Zeiss LEO EVO 50XVP electron microscope equipped with an Oxford Instruments EDX INCA Energy 450 analyzer. For each element in Ce$_2$RuAl, the uncertainty of detection did not exceed 0.9 at.%. The result yielded the sample composition 50.4 at.% Ce, 24.9 at.% Ru, and 24.7 at.% Al, in good agreement with the chemical formula Ce$_2$RuAl.

2.3. Single crystal X-ray data

Small single crystals suitable for X-ray data collection were isolated from the polycrystalline ingot of Ce$_2$RuAl by mechanical fragmentation. The single-crystal X-ray diffraction data were collected with a Bruker APEX-II four-circle diffraction system equipped with a CCD detector (Mo Kα radiation, graphite monochromator). The X-ray intensities were empirically corrected for absorption using the SADABS program [27]. The observed systematic extinctions led to the non-centrosymmetric space group $P6_3cm$. The reliability of this space group was confirmed during the structure refinement and ensured using the PLATON program [28]. The structure refinement (full-matrix least-squares on F^2 with anisotropic displacement parameters for all atoms) was performed employing the SHELX-97 program package [29]. The correctness of the final structural model was ensured through calculation of the

* Corresponding author. Fax: +7 495 9390171.
  E-mail address: murashovaev@rambler.ru (E. Murashova).

Flack parameter [30]. Details on the data collection and their analysis are summarized in Table 1. The atomic parameters and the main interatomic distances are listed in Tables 2 and 3, respectively. Further crystallographic information can be obtained from Fachinformationszentrum Karlsruhe, D-76344 Eggenstein–Leopoldshafen, Germany on quoting the deposition number CSD-422577.

2.4. X-ray powder diffraction

Powder X-ray diffraction (XRD) pattern was measured with a STOE STADI P transmission diffractometer equipped with a Cu-tube, a curved Ge (1 1 1) primary-beam monochromator and a linear PSD detector. The experimental conditions were: angle range $5° < 2\theta < 105°$, step scan $0.01°$, and 10 s counting time per point. The measured powder diffraction pattern was indexed within a primitive hexagonal unit cell using the program TREOR [31]; $F(43) = 77$. Moreover, it was subjected to Rietveld profile fitting performed employing the FULLPROF program [32]. The results fully corroborated the structural model derived from the single-crystal XRD data.

2.5. Thermal analysis

Differential scanning calorimetric (DSC) measurements were carried out on a small (1.8 mg) polycrystalline sample of Ce_2RuAl employing a NEITZCH STA 449 F1 Jupiter Platinum RT analyzer. Heating was performed from 298 K to 900 K with a rate of 10 K/min in high-purity helium atmosphere. No hint at any structural phase transition was found up to the melting point occurring at 897(1) K.

2.6. XANES spectroscopy

The electronic structure of Ce_2RuAl was studied by means of X-ray Absorption Near Edge Structure (XANES) spectroscopy. The L_3-Ce absorption edge spectra were collected at A1 beamline of the DORIS III positron storage ring at DESY/HASYLAB (Hamburg, Germany) in transmission mode at room temperature. Energy resolution of the double-crystal Si (1 1 1) monochromator (detuned to reject 50% of the incident signal in order to minimize harmonic contamination) with a 0.3 mm slit at 6 keV was about 1.2 eV.

Table 1
Crystal data and details on structural refinement for Ce_2RuAl.

Empirical formula	Ce_2RuAl
Molar mass (g/mol)	408.29
Structure type, Pearson symbol	Ce_2RuAl, hP24
Space group (Z)	$P6_3cm$ (No. 185), 6
Unit cell dimensions a, c (Å)	7.8362(7), 9.7510(9)
V (Å^3), Calculated density (g/cm^3)	518.55(8), 7.85
Crystal size (mm)	$0.15 \times 0.12 \times 0.08$
T (K)	293(2)
Radiation, λ (Å)	Mo Kα, 0.71073
Absorption coefficient (mm^{-1})	30.164
$F(000)$	1038
θ range (°)	3, 37.47
Range in hkl	$-11 \div 13$; $-12 \div 5$; $-16 \div 15$
Total no. reflections	4943
Independent reflections (R_{int})	987 (0.033)
Reflections with $I > 2\sigma(I)$ (R_σ)	952 (0.027)
Refined parameters no.	26
Goodness-of-fit on F^2	1.024
Final R indices $[I > 2\sigma(I)]$ $R1$	0.017
$wR2$	0.035
R indices (all data) $R1$	0.019
$wR2$	0.036
Extinction coefficient	0.00487(17)
Flack parameter	0.04(2)
Largest diff. peak and hole, e (Å^3)	1.780/−0.894

Table 2
Atomic coordinates and displacement parameters (Å^2) for Ce_2RuAl.

Atom	Multiplicity, Wyckoff letter	x/a	y/b	z/c	U_{eq}
Ce1	6c	0	0.41161(4)	0.00000(2)	0.01003(6)
Ce2	6c	0	0.26137(4)	0.32406(3)	0.01032(6)
Ru	6c	0	0.65869(5)	0.15928(6)	0.00892(7)
Al1	4b	1/3	2/3	0.2294(2)	0.0097(3)
Al2	2a	0	0	0.0769(3)	0.0092(4)

Table 3
Interatomic distances (Å) in the unit cell of Ce_2RuAl.

Atom1	Atom2	Distance
Ce1	Ru	2.4821(6)
	Ce2	3.0839(4)
	2Al1	3.2558(14)
	2Ce2	3.3069(3)
	Al2	3.3114(8)
	3Ru	3.3677(7)
	Ce2	3.3721(4)
	Average	3.2253
Ce2	2Ru	2.9072(5)
	2Al1	3.0767(7)
	Ce1	3.0839(4)
	Al2	3.163(2)
	Al2	3.205(2)
	2Ce1	3.3069(3)
	Ru	3.3283(7)
	Ce1	3.3721(4)
	Average	3.1576
Ru	Ce1	2.4821(6)
	2Al1	2.6704(6)
	Al2	2.7928(10)
	2Ce2	2.9072(5)
	Ce1	3.3677(7)
	2Ce1	3.3679(4)
	Ce2	3.5036(6)
Al1	3Ru	2.6704(6)
	3Ce2	3.0767(7)
	3Ce1	3.2558(14)
Al2	3Ru	2.7928(10)
	3Ce2	3.163(2)
	3Ce2	3.205(2)

2.7. Physical measurements

Magnetic studies were performed in the temperature range 4.2–400 K in magnetic fields up to 5 T using a Quantum Design MPMS magnetometer. The electrical resistivity was measured over the interval 4.2–300 K by a standard DC four-point method employing a home-made setup. The current and voltage leads were attached to a bar-shaped specimen using silver epoxy paste.

3. Results and discussion

3.1. Crystal structure

The Rietveld refinement of the powder X-ray diffraction pattern of Ce_2RuAl (see Fig. 1) yielded a residual value of $R_F = 0.046$ for 138 inequivalent contributing reflections ($\chi^2 = 3.77$, $R_B = 0.068$, $wR_P = 0.033$, $R_{exp} = 0.025$). The so-obtained hexagonal lattice parameters are: $a = 7.8320(2)$ Å and $c = 9.7450(2)$ Å, i.e. they are close to those refined from the single crystal data: $a = 7.8362(7)$ Å and $c = 9.7510(9)$ Å (Table 1). No secondary phases were detected on the XRD pattern.

The crystal structure of Ce_2RuAl is of a new type, which can be related to the structure of LaF_3 ($Z = 6$, $P6_3cm$) [33] that was reported for a few binary intermetallics: Mg_3Pd [34], Mg_3Rh [35], Mg_3T (T = Pt, Ir, Au) [36,37]. In the unit cell of LaF_3, the atoms are distributed over five crystallographically independent positions: one La(6c), two F(6c), one F(4b), and one F(2a). In Ce_2RuAl, the Ru atoms are located at the 6c site, whereas the other constituents selectively occupy the F sites, namely two Al atoms are placed at the 4b and 2a positions, and two Ce atoms fill both the 6c positions. It appears that Ce_2RuAl is the first representative of this type of atom arrangement among ternary intermetallics.

In the unit cell of Ce_2RuAl, the nearest environment of the two independent Ce atoms consists of 11 atoms placed at distances up to 3.38 Å. The coordination polyhedra Ce1[$Ce_4Ru_4Al_3$] and Ce2[$Ce_4Ru_3Al_4$] are displayed in Fig. 2a and b, respectively. The average dis-
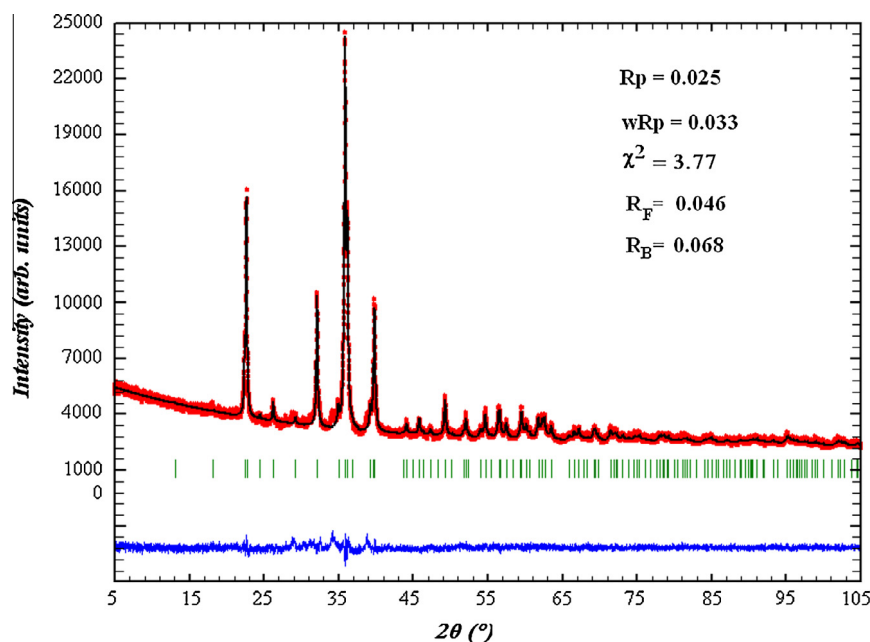
Fig. 1. Experimental, calculated, and difference powder X-ray diffraction patterns of Ce$_2$RuAl. The vertical bars indicate the Bragg peak positions.

tance between the Ce1 atom and its neighbors (Ru, Al, Ce2) is 3.2253 Å. Most remarkably, in the Ce1 polyhedron, the shortest Ce–Ru distance amounts to 2.4821(6) Å, i.e. it is significantly smaller than the sum of the covalent radii of cerium and ruthenium. As mentioned in the Introduction, such an anomalously short Ce1–Ru contact may reflect an intermediate valence state of the Ce1 ion. Indeed, the physical property measurements of Ce$_2$RuAl positively proved this conjecture (see below). In the Ce2 polyhedron, the nearest Ru neighbors are placed at a distance of 2.9072(5) Å that is close to the sum of the respective covalent radii. The average distance between Ce2 and the surrounding atoms (Ru, Al, Ce1) is equal to 3.1546 Å, being thus significantly shorter than that in the Ce1 polyhedron.

In the first coordination sphere (up to 2.91 Å) of the Ru atom, there are three Ce atoms and three Al atoms, which jointly form a distorted trigonal prism Ru[Ce$_3$Al$_3$] (see Fig. 2c). Four Ce atoms from the second coordination sphere of Ru are placed at distances ranging from 3.3677(7) Å to 3.5036(6) Å. Both crystallographically independent Al atoms have nine adjacent atoms. They outline a tricapped trigonal prism [Ce$_6$Ru$_3$] around Al1 (Fig. 2d) and a tricapped trigonal antiprism [Ce$_6$Ru$_3$] in the case of the Al2 atom (Fig. 2e).

The crystal structure of Ce$_2$RuAl has a layered character and can be presented as an assembly of the Ru polyhedra, which share edges and corners (see Fig. 3a and b). The layers alternate along the [0 0 1] direction that is related to the 6$_3$ axis. As displayed in

Fig. 3d, the particular layers are constructed in such a way that the Al and Ru atoms located inside the layer form a corrugated hexagonal network, and the Ce atoms are placed at the borders of the layer. The interatomic distances between the Ru atoms and their nearest neighbor Al atoms within the layers range from 2.6704(6) Å to 2.7928(10) Å. The Ce atoms of two adjacent layers form a strongly corrugated hexagonal network (see Fig. 3c) with the interatomic Ce–Ce distances ranging from 3.0839(4) to 3.3069(3) Å. The shortest interlayer contact occurs between the Ce1 and Ce2 atoms (3.0839(4) Å).

3.2. Physical properties

Fig. 4 displays the XANES spectrum recorded for Ce$_2$RuAl at the Ce-L_3 absorption edge at room temperature. The maximum is split into two features, which clearly arise due to Ce^{3+} and Ce^{4+} contributions. This finding implies the presence of a homogeneous intermediate valence state or a heterogeneous mixed valence state of the cerium ions in the compound studied. The evaluation of the experimental spectra was performed using the conventional fitting of absorption peaks with combinations of Lorentzian, Gaussian and arctangent curves of constrained widths and energy positions [38]. As can be inferred from Fig. 4, the proper description was obtained with just two spectral contributions corresponding to the 4f^1 (Ce^{3+}) and 4f^0 (Ce^{4+}) states. The so-derived Ce valence amounts to υ = 3.19. This value is an average valence of all the cerium ions dis-
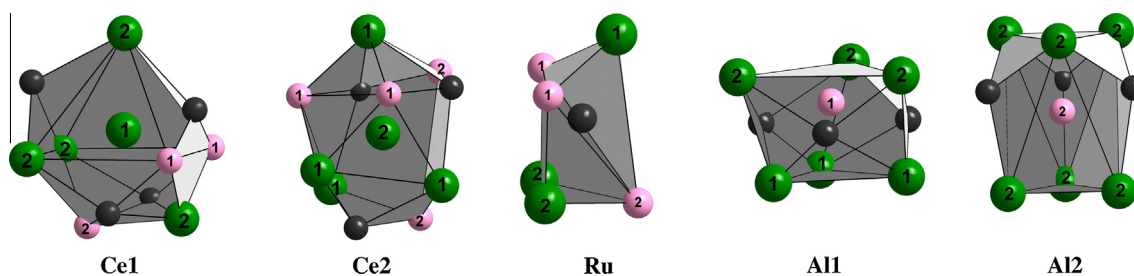

Fig. 2. Coordination polyhedra of the Ce (a and b), Ru (c) and Al (d and e) atoms in the unit cell of Ce$_2$RuAl.
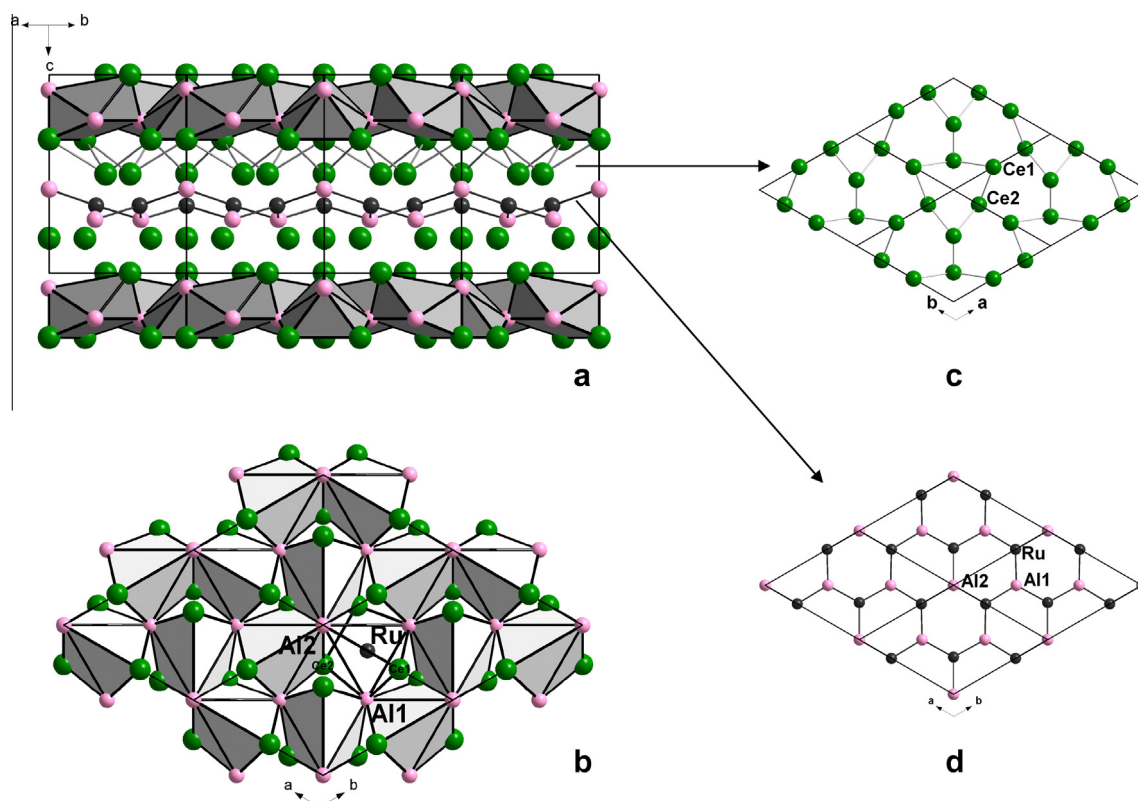
Fig. 3. Projection of the crystal structure of Ce_2RuAl along the [110] direction (a). Single layer of the Ru polyhedra oriented perpendicular to the [001] direction (b). Corrugated hexagonal networks of the Ce atoms (c) and of the Ru and Al atoms (d).
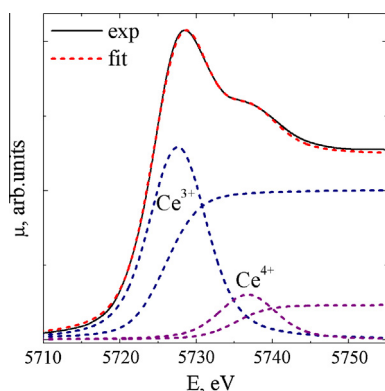

Fig. 4. XANES L_3-Ce absorption edge spectrum of Ce_2RuAl and its deconvolution into components.

tributed over the Ce1 and Ce2 positions, and its large magnitude suggests that all these ions possess unstable 4f-shell. However, taking into account the structural features, namely the unusually short Ce1–Ru distances, one might speculate that the Ce1 ions in Ce_2RuAl exhibit much stronger deviation from the trivalent state than the Ce2 ions.

In line with the XANES data, the magnetic susceptibility of Ce_2RuAl depends on temperature in a manner typical for intermediate valence systems [39,40]. As shown in Fig. 5, in the entire temperature range covered the molar susceptibility is small and clearly of non-Curie–Weiss type. A gradual decrease in $\chi^{-1}(T)$, seen above 250 K, hints at the presence of a IV-type susceptibility minimum [15] occurring in the compound studied at $T(\chi_{max}) > 400$ K. Here it is worthwhile recalling that for example in the intermediate-valent gallides $Ce_2Ru_2Ga_3$ [25] and $Ce_4Ru_3Ga_3$ [24] $T(\chi_{max})$ amounts to about 150 K and 250 K, respectively, however for the

closely related IV compound $Ce_9Ru_4Ga_5$ [23] as well as for the IV aluminide $Ce_5Ru_3Al_2$ [7] $T(\chi_{max})$ significantly exceeds 400 K. As $T(\chi_{max})$ is a measure of the characteristic energy scale of valence fluctuations [15], its large magnitude is in concert with the large mean Ce valence value derived for Ce_2RuAl from the XANES data. Moreover, the observed magnetic behavior supports the presumption of both Ce1 and Ce2 ions having unstable 4f shells.

A striking feature of Ce_2RuAl, rather unusual for strongly intermediate valence systems, is a small maximum in $\chi(T)$ occurring near 10 K (see the right-hand side inset to Fig. 5). This anomaly, taken together with a metamagnetic-like inflection in the magnetic field variation of the magnetization measured much below 10 K and a fairly large magnitude of the magnetization found in strong
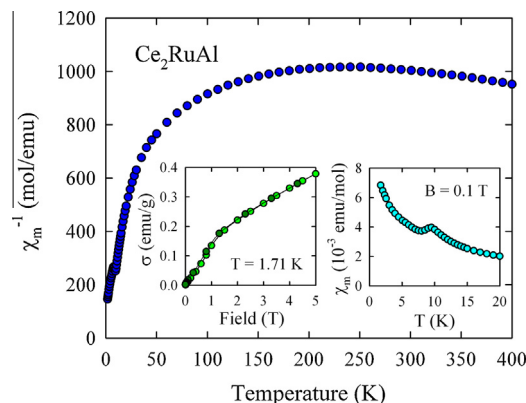

Fig. 5. Temperature dependence of the reciprocal molar magnetic susceptibility of Ce_2RuAl measured in a field of 0.1 T. The right-hand side inset shows the low-temperature magnetic susceptibility data. The other inset presents the magnetization of Ce_2RuAl measured at 1.71 K as a function of magnetic field with increasing (full symbols) and decreasing (open symbols) field strength.
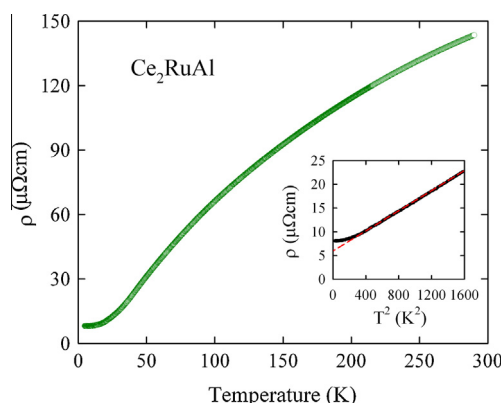
Fig. 6. Temperature variation of the electrical resistivity of Ce$_2$RuAl. The inset displays the low temperature data as a function of squared temperature. The dashed line emphasizes a straight line behavior.

magnetic fields (see the other inset to Fig. 5), might be considered as an indication of antiferromagnetic ordering setting in at low temperatures. Though the coexistence of a long-range magnetic order and valence fluctuations has been reported in the literature for a few Ce–Ru–X compounds, like Ce$_9$Ru$_4$Ga$_5$ (antiferromagnetic transition at 3.7 K) [23], Ce$_{23}$Ru$_7$Cd$_4$ (ferro- or ferromagnetic order below 3.6 K) [16], Ce$_{23}$Ru$_7$Mg$_4$ (antiferromagnetic state below 2.9 K) [41], and Ce$_2$RuZn$_4$ (probable ordering below 2 K) [15], such a scenario seems unlikely in the case of Ce$_2$RuAl because the "antiferromagnetic" anomaly in $\chi(T)$ is relatively weak, and what's more, no corresponding singularity is observed in the electrical resistivity data (see below). Definitively at odds with the hypothetical magnetic ordering is the intermediate valent character of all the Ce ions in the material studied. This situation is essentially different from that inferred e.g. for Ce$_9$Ru$_4$Ga$_5$ in which 1/3 of the Ce ions in the crystallographic unit cell has a stable trivalent state that yields antiferromagnetic ordering evidenced in all the key bulk properties of the compound: magnetic susceptibility, heat capacity and electrical resistivity [23]. For these reasons, the low-temperature magnetic future in Ce$_2$RuAl should be tentatively ascribed to unknown magnetic impurity, present in the measured sample in an amount below the detection limit of powder X-ray diffraction and probably overlooked in the performed EDXS examination.

The temperature dependence of the electrical resistivity of Ce$_2$RuAl is shown in Fig. 6. The compound exhibits a good metallic-like conductivity with strongly curved $\rho(T)$ over the temperature range covered. At room temperature, the resistivity amounts to $\rho_{300K} = 144\ \mu\Omega$ cm, and at 4.2 K it saturates at a value $\rho_{4.2K} = 8\ \mu\Omega$ cm. The large residual resistivity ratio $\rho_{300K}/\rho_{4.2K} = 18$ indicates a quite high quality of the polycrystalline sample investigated. Generally, the electrical resistivity of intermediate valence systems is governed mainly by scattering conduction electrons on structural defects, lattice vibrations and spin fluctuations. For Ce$_2$RuAl, which bears two sublattices of the Ce ions having notably different effective occupancies of the electronic 4f shell, no reliable numerical analysis of the experimental data in wide temperature range seems possible. It is however worthwhile noting that below about 40 K, the resistivity is proportional to the squared temperature. Such a Fermi liquid behavior of $\rho(T)$ is a characteristic feature of IV systems [42]. This functional dependence of the resistivity breaks down at the lowest temperatures studied (below ca. 13 K), possibly because of the impurities revealed in the magnetic studies.

4. Conclusions

The new aluminide Ce$_2$RuAl crystallizes with its own type hexagonal crystal structure derived from the LaF$_3$ type. The compound is a novel representative of the ternary intermetallics with anomalously short Ce–Ru distances. This structural feature is associated with an intermediate valence state of the Ce atoms involved. At room temperature, the mean Ce valence amounts to about 3.19, as derived from the X-ray absorption spectroscopy near the cerium L_3-edge. The strongly unstable character of the electronic 4f-shell of the Ce ions manifests itself in the characteristic low-temperature dependencies of the magnetic susceptibility and the electrical resistivity of Ce$_2$RuAl.

Acknowledgments

References

[1] A.I. Tursina, S.N. Nesterenko, E.V. Murashova, I.V. Chernyshev, H. Noel, Y.D. Seropegin, Acta Cryst. E 61 (2005) i12–i14.
[2] A.I. Tursina, S.N. Nesterenko, E.V. Murashova, I.V. Chernyshev, H. Noel, Y.D. Seropegin, Acta Cryst. E 60 (2004) i145–i146.
[3] N.G. Bukhan'ko, A.I. Tursina, S.V. Malyshev, A.V. Gribanov, Y.D. Seropegin, O.I. Bodak, J. Alloys Comp. 367 (2004) 149–151.
[4] A.I. Tursina, N.G. Bukhan'ko, A.V. Gribanov, H. Noel, T. Roisnel, Y.D. Seropegin, J. Alloys Comp. 400 (2005) 194–196.
[5] C. Schank, F. Jahrling, L. Luo, A. Grauel, C. Wassilew, R. Borth, G. Olesch, C.D. Bredl, C. Geibel, F. Steglich, J. Alloys Comp. 207 (1994) 329–332.
[6] T. Mishra, R.-D. Hoffmann, C. Schwickert, R. Pöttgen, Z. Naturforsch. 66b (2011) 771–777.
[7] E.V. Murashova, A.I. Tursina, N.G. Bukhanko, S.N. Nesterenko, Zh.M. Kurenbaeva, Y.D. Seropegin, H. Noël, M. Potel, T. Roisnel, D. Kaczorowski, Mater. Res. Bull. 45 (2010) 993–999.
[8] A.V. Gribanov, A.I. Tursina, A.V. Grytsiv, E.V. Murashova, N.G. Bukhan'ko, P. Rogl, Y.D. Seropegin, G. Giester, J. Alloys Comp. 454 (2008) 164–167.
[9] W. Hermes, S.F. Matar, R. Pöttgen, Z. Naturforsch. 64b (2009) 901–908.
[10] Zh.M. Kurenbaeva, E.V. Murashova, D.N. Hannanov, A.B. Ilyukhin, A.I. Tursina, Yu.D. Seropegin, Ternary intermetallics La4RuAl, Ce4RuAl, and Ce4RuIn, in: Collected Abstracts of the XI International Conference on Crystal Chemistry of Intermetallic Compounds (XI IMC), Lviv, Ukraine, 2010, p. 103.
[11] F. Tappe, Ch. Schwickert, S. Linsinger, R. Pöttgen, Monatsh. Chem. 142 (2011) 1087–1095.
[12] E.V. Murashova, A.I. Tursina, Zh.M. Kurenbaeva, H. Noël, Y.D. Seropegin, Chem. Met. Alloy. 3 (2010) 101–107.
[13] J. Emsley, The Elements, Clarendon Press, Oxford, 1989.
[14] J.F. Riecken, W. Hermes, B. Chevalier, R.-D. Hoffmann, F.M. Schappacher, R. Pöttgen, Z. Anorg. Allg. Chem. 633 (2007) 1094–1099.
[15] R. Mishra, W. Hermes, U.Ch. Rodewald, R.-D. Hoffmann, R. Pöttgen, Z. Anorg. Allg. Chem. 634 (2008) 470–474.
[16] F. Tappe, W. Hermes, M. Eul, R. Pöttgen, Intermetallics 17 (2009) 1035–1040.
[17] Zh.M. Kurenbaeva, A.I. Tursina, E.V. Murashova, S.N. Nesterenko, A.V. Gribanov, Yu.D. Seropegin, H. Noël, J. Alloys Comp. 442 (2007) 86–88.
[18] E.V. Murashova, Zh.M. Kurenbaeva, A.I. Tursina, H. Noël, P. Rogl, A.V. Grytsiv, A.V. Gribanov, G. Giester, Yu.D. Seropegin, J. Alloys Comp. 442 (2007) 89–92.
[19] A.I. Tursina, Zh.M. Kurenbaeva, A.V. Gribanov, H. Noël, T. Roisnel, Y.D. Seropegin, J. Alloys Comp. 442 (2007) 100–103.
[20] E.V. Murashova, A.I. Tursina, Zh.M. Kurenbaeva, A.V. Gribanov, Yu.D. Seropegin, J. Alloys Comp. 454 (2008) 206–209.
[21] Zh.M. Kurenbaeva, A.I. Tursina, E.V. Murashova, S.N. Nesterenko, Yu.D. Seropegin, Russ. J. Inorg. Chem. 56 (2011) 218–222.
[22] K. Shablinskaya, E. Murashova, A. Tursina, Zh. Kurenbaeva, A. Yaroslavtsev, Y. Seropegin, Intermetallics 23 (2012) 106–110.
[23] D. Kaczorowski, E. Murashova, Z. Kurenbaeva, J. Alloys Comp. 557 (2013) 23–26.
[24] K. Shablinskaya, E. Murashova, Zh. Kurenbaeva, A. Yaroslavtsev, Yu. Seropegin, D. Kaczorowski, J. Alloys Comp. 575 (2013) 183–189.
[25] E. Murashova, K. Shablinskaya, Zh. Kurenbaeva, A. Yaroslavtsev, A. Menushenkov, R. Chernikov, O. Grishina, S. Nesterenko, Yu. Seropegin, D. Kaczorowski, Intermetallics 38 (2013) 23–29.
[26] S.F. Matar, B. Chevalier, R. Pöttgen, Intermetallics 31 (2012) 88–93.
[27] G.M. Sheldrick, SADABS – Bruker Nonius area detector scaling and absorption correction, University of Göttingen, Germany, 2004.
[28] A.L. Spek, J. Appl. Crystallogr. 36 (2003) 7–13.

[29] G.M. Sheldrick, Acta Crystallogr. A 64 (2008) 112–122.

[30] H.D. Flack, Acta Crystallogr. A 39 (1983) 876–881.

[31] STOE WinXPow, version 2.24, STOE & Cie GmbH: Darmstadt, Germany, 2009.

[32] J. Rodriguez-Carvajal, Commission Powder Diffr. (IUCr) 26 (2001) 12–19.

[33] C. De Rango, G. Tsoucaris, C. Zelwer, Sci. Chim. 263 (1966) 64–66.

[34] J.P.A. Makongo, C. Kudla, Yu. Prots', R. Niewa, U. Burkhardt, G. Kreiner, Z. Kristallogr. 220 (2005) 289–290.

[35] V. Hlukhyy, U.C. Rodewald, R.D. Hoffmann, R. Pöttgen, Z. Naturforsch. 59 (2004) 251–255.

[36] K.J. Range, P. Hafner, J. Alloys Comp. 183 (1992) 430–437.

[37] K.J. Range, P. Hafner, J. Alloys Comp. 191 (1993) 5–7.

[38] J. Röhler, J. Magn. Magn. Mater. 47–48 (1975) 175–180.

[39] J.M. Lawrence, P.S. Riseborough, R.D. Parks, Rep. Prog. Phys. 44 (1981) 1–84.

[40] D. Kaczorowski, P. Rogl, K. Hiebl, Phys. Rev. B 54 (1996) 9891–9902.

[41] S. Linsinger, M. Eul, W. Hermes, R.-D. Hoffmann, R. Pöttgen, Z. Naturforsch. 64b (2009) 1345.

[42] D. Wohlleben, B. Wittershagen, Adv. Phys. 34 (1985) 403–443.